



Investigation of New IPM Linear Machine Configuration with Low Permanent Magnet Used

Ahlam L. Shurajji ^{a*}, Nattapong Pothi ^b, Hashmia Sh. Dakeel ^c

^a Department of Electromechanical Engineering, University of Technology-Iraq.
50053@uotechnology.edu.iq

^b Department of Electrical Engineering School of Engineering, University of Phayao, Phayao, Thailand,
nattapong.po@up.ac.th

^c Department of Electromechanical Engineering, University of Technology-Iraq.

* Corresponding author

Submitted: 17/06/2019

Accepted: 24/08/2019

Published: 25/06/2020

KEY WORDS

Cogging force, Force ripple, PM linear machine, PM utilization

ABSTRACT

Permanent magnet (PM) machines have received numerous attentions, since they are distinguished by many desirable features including simple construction and high efficiency. However, high price of the permanent magnet material may be considered as the main problems of such machines. Hence, the demand of PM machine with high efficient PM materials used is increased. In this study a new configuration of PM linear machine with high efficient PM material utilization, named as V-shape interior PM linear machine is investigated. The mentioned machine has been compared to the conventional I-shape counterpart. In order to perform sensible comparison, I-shape and V-shape machines have been designed with identical main design specifications. It has been observed that the V-shape topology shows better PM material utilization. It should be noted that about 43% higher efficient PM used is obtained by the V-shape machine compared to the conventional I-shape corresponding. It should be noted that the V-shape machine has been designed with about 51.6% less total permanent magnet volume compared to I-shape machine. Moreover, the introduced machine offers less cogging force as well as thrust force ripple than that of the conventional machine.

How to cite this article: A.L. Shurajji, N. Pothi and H. Sh. Dakeel, "Investigation of new IPM linear machine configuration with low permanent magnet used," *Engineering and Technology Journal*, Vol. 38, Part A, No. 06, pp. 825-831, 2020.

DOI: <https://doi.org/10.30684/etj.v38i6A.354>

This is an open access article under the CC BY 4.0 license <http://creativecommons.org/licenses/by/4.0>

1. Introduction

Linear electromagnetic machines have become promising candidates for direct drive applications, due to high system efficiency as well as reliability resulting from the absent of rotary to linear conversion mechanism that must be presented when using rotary machines [1-3]. Among various types of linear machines, permanent magnet linear machines (PMLMs) are being of interesting, since they offer the advantage of high output thrust force and consequently high efficiency [4-7].

Regarding PM machines, interior permanent magnet machines (IPMMs) are more preferable compared to surface mounted permanent magnet machines (SPMMs), due to the fact that IPMMs deliver high output torque, thanks to contribution of both PM and reluctance torque to the output torque of such machines [8-9].

IPMMs can be designed with I-shape, spoke-shape and V-shape PM structures. Due to the high prize of the PM material, proper utilize of such material has been an important issue in PM machine design. As rotary V-shape PM machines possess better PM utilization compared to the other types of rotary IPMMs [10], they have been widely discussed in literature. In contrast, linear V-shape PM machine has not been investigated yet. Hence, in order to investigate the benefit of such configuration in linear machine topology, a new PM linear machine with V-shape construction is introduced in this study based on the rotary V-shape PM machine. The machine description is shown in section 2. On the other hand, section 3 presents global optimization for maximum average thrust force, while a comparison between I-shape IPM linear machine and the proposed machine is introduced in section 4. Moreover, the conclusion is given in section 5.

2. Machine Configuration

I-shape and V-shape IPM machines are shown in Figure 1. It must be mentioned that for fair comparison, the understudying machines are designed with the same specifications, which are illustrated in Table 1. The machines have 12/10 stator/mover combination with concentrated windings, which are preferable for the advantage of low copper loss and consequently efficiency enhancement. Furthermore, additional teeth have been added in both left and right ends of the stators of both machines, to reduce cogging force [11].

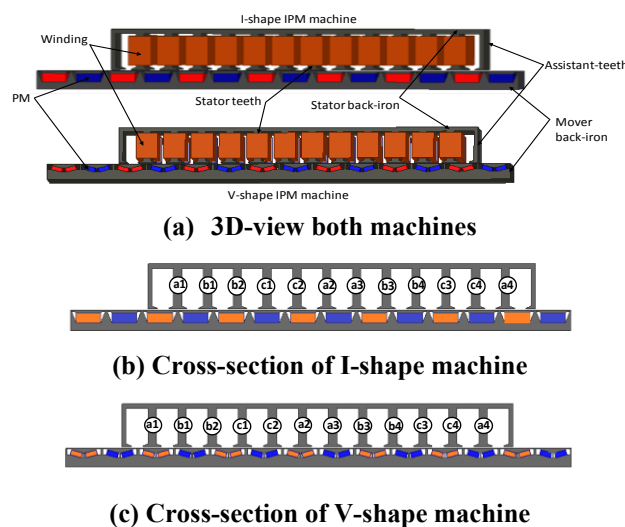


Figure 1: Machines layouts

3. Average Thrust Force Optimization

In order to deliver maximum average thrust force, global optimizations using finite element based genetic algorithm have been conducted for both machines. All the parameters that are listed in Table 1 have not been changed during the optimization. In contrast, Table 2 shows restriction and optimal values of the changing parameters during the optimization. Moreover, schematics of the mentioned parameters are demonstrated in Figure 2. It can be clearly observed that the understudying machines have the same stator optimal dimensions and the same split ratio. On the other hand, each machine has different dimensions for PM and mover back-iron. It should be noted that machines configurations with optimal dimensions are shown in Figure 1.

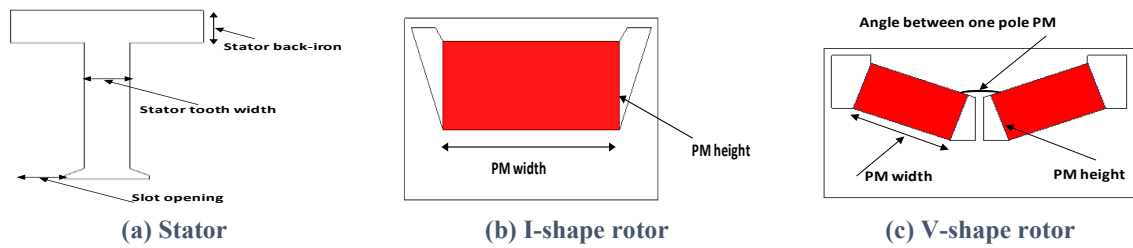


Figure 2: Changing parameters through optimization

Table 1: Main specifications of both machines

Parameters	Values
Air-gap	0.75 mm
Active-length	198 mm
Pole-number of stator	12
Pole-number of mover	10
Machine-depth	25 mm
Machine-height	35 mm
Slot-pitch	16.5 mm
Pole-pitch	19.8 mm
Copper loss	25 W
Number of turn/coil	30
Number of coil/phase	4
Number of phases	3

Table 2: Changing parameters during optimization

Parameters	restrictions	Optimal
Split-ratio	0.2-0.5	0.3
Stator-tooth width	(3-6) mm	4.5 mm
Slot-opening width	(1.5-4.5) mm	3.23 mm
Stator back-iron	(1.5-5) mm	2.5 mm
PM height (I-shape)	(2-7) mm	5.15 mm
PM width (I-shape)	(5-15) mm	7 mm
PM height (V-shape)	(0.1-0.35) mm	0.26 mm
PM width (V-shape)	(1.5-4.5) mm	3.22 mm
Angle between the PM (V-shape)	(140-180) degrees	162 degree

4. Performance Analysis

After optimization, the performances of understudying machines including no-load and on-load conditions are analyzed by 2D-FEA. Flux distributions when the mover moves one pole pitch at no-load condition are illustrated in Figure 3. Comparisons of three-phase flux linkage and back-EMF of both understudying machines are presented in Figures 4-5, respectively. Clearly, both machines have a symmetrical three phase flux linkage waveforms, because of the longitudinal end effect that is inherent feature of linear machine configuration. It can be seen that higher flux linkage is for I-shape machine, due to the larger PM volume. Moreover, back-EMF waveforms for both machines contain third harmonic order. Notably, I-shape PM topology has higher back-EMF compared to V-shape topology, as the former has higher flux linkage. In addition, Figure 6 compares cogging force of both machines. Linear PM machines generally suffer higher cogging force than the rotary corresponding, since cogging force is caused by the interaction between the PM and stator teeth as well as the longitudinal end effect at no-load operation. Apparently, V-shape topology has slightly lower

cogging force than that of the I-shape topology. Besides, average thrust force variations with current angle are shown in Figure 7. The optimal current angle for I-shape and V-shape PM machines is 10 and 15 degrees, respectively. Figure 8 illustrates thrust force waveforms with mover position when the mover moves one pole pitch, while the average values of such force for both machines are compared in Figure 9. Obviously, higher average thrust force is for I-shape topology. In addition, Figure 10 depicts thrust force ripple for understudying machines. It can be noted that less thrust force ripple is obtained by V-shape machine. Moreover, the characteristics of average thrust force against copper loss for the understudying machines are presented in Figure 11, both machines have the same trend, i.e., at the low values of copper loss the changing of thrust force is almost linear and at high value of copper loss the variation becomes non-linear, because of the saturation of the ferromagnetic material. In order to investigate the PM used efficiency, the average thrust force per total PM volume versus different copper loss values are shown in Figure 12 for both machines. It can be clearly noted that V-shape machine has better PM utilization compared to the I-shape machine. The performances of both machines are summarised in Table 3. It can be observed that I-shape topology shows higher flux linkage, back-EMF and average thrust force by about 12.3%, 13.7% and 13.87% compared to the V-shape machine, as the former has larger PM volume than the latter. On the other hand, lower cogging force as well as thrust force ripple and more efficient used of the PM material are delivered by V-shape configuration.

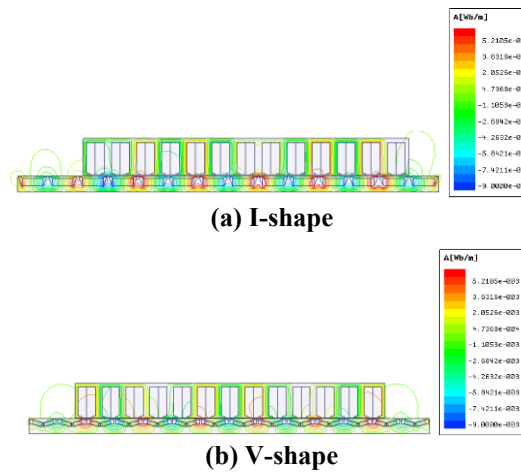
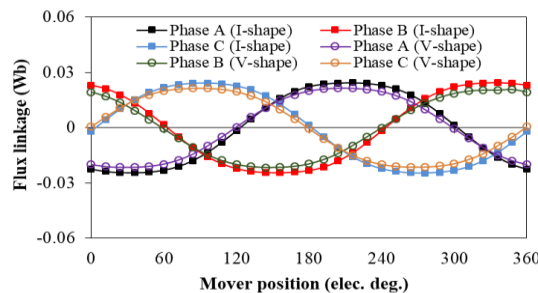
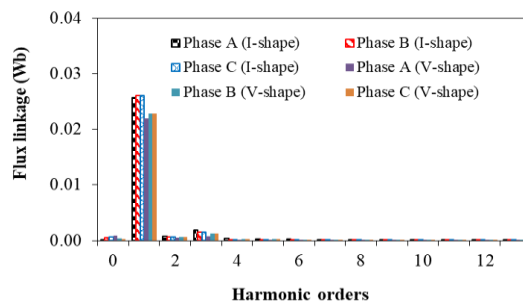


Figure 3: Flux-lines distributions of the understudying machines

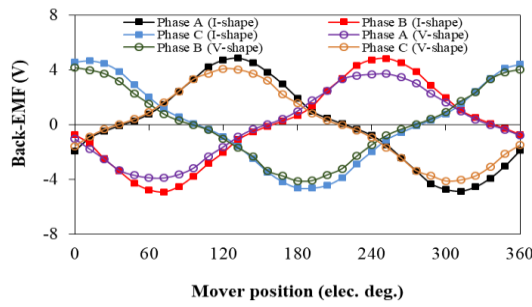


(a) Flux-linkage waveforms

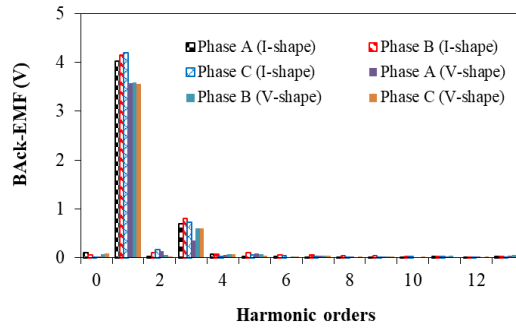


(b) FFT of Flux-linkage

Figure 4: Flux-linkage and FFT of the understudying machines



(a) Back-EMF waveforms



(b) FFT of back-EMF

Figure 5: Back-EMF and FFT of the understudying machines

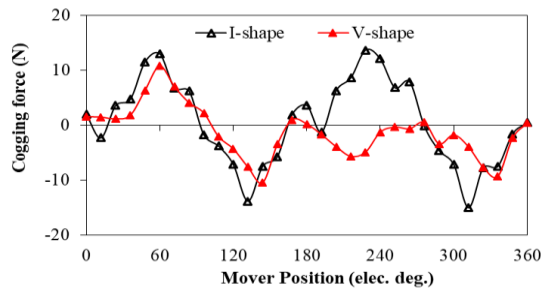


Figure 6: Cogging force of the understudying machines

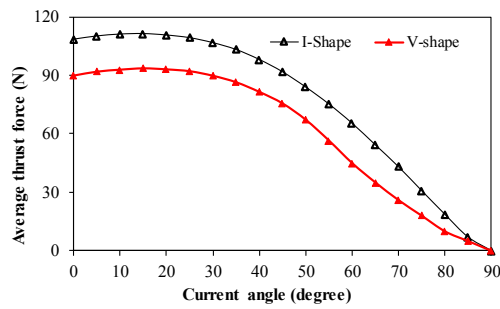


Figure 7: Average thrust force versus current angle of the understudying machines

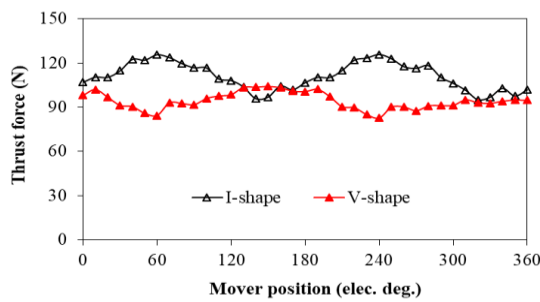


Figure 8: Thrust force of the understudying machines

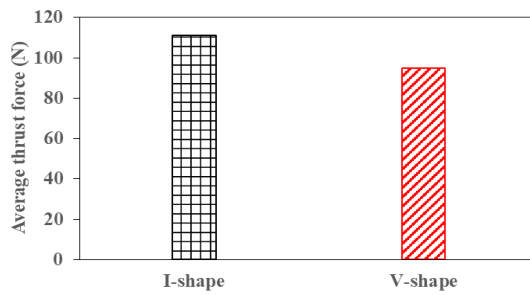


Figure 9: Average thrust force of the understudying machines

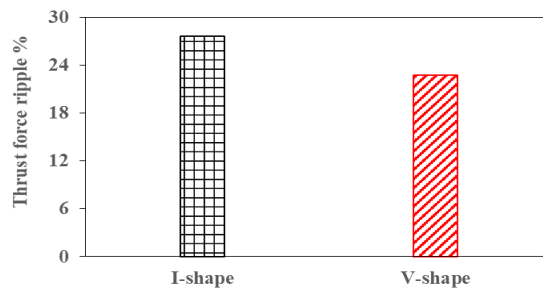


Figure 10: Thrust force ripple of the understudying machines

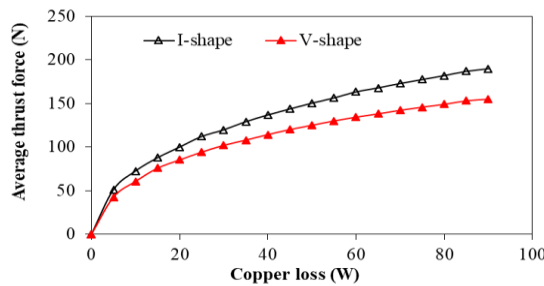


Figure 11: Thrust force versus copper loss of the understudying machines

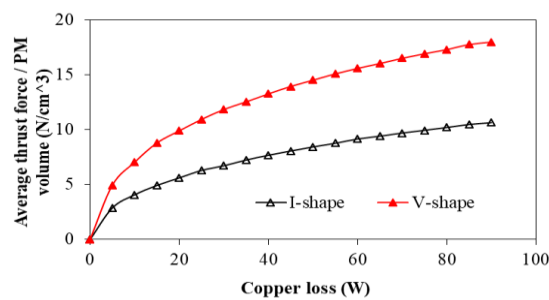


Figure 12: PM utilization of the understudying machines

Table 3: Performance comparison of both machines

Items	I-shape machine	V-shape machine
Phase flux-linkage (Wb)	0.0244	0.0214
Phase back-EMF (V)	4.87	4.21
Cogging force peak value (N)	13.7	10.8
Average thrust force (N)	111	95.6
Thrust force ripple	27%	22%
Total PM volume (cm ³)	17.8	8.6
Average thrust force per PM volume (N/ cm ³)	6.23	11.1

5. Conclusion

Seeking for PM linear machine with high efficient PM material utilization, an IPM linear machine with a new PM configuration named as V-shape IPM linear machine has been investigated in this paper. The machine is designed, optimized and analyzed using 2D-FEA. It must be noted that the used 2D-FE package is (ANSYS-Maxwell 16.0). To evaluate the performance of the mentioned machine, a comparison between such machine and the existing I-shape IPM linear machine is carried out under the same design and optimization circumstances. It is revealed that the V-shape topology delivers lower cogging force as well as thrust force ripple and about 43% higher PM material utilization than the conventional I-shape topology. Thereby, it can be deduced that the V-shape IPM machine can be a potential candidate for many applications, particularly when the cost of the machine is a crucial issue. This is because the total PM volume in V-shape configuration has been reduced to about 51.6% with comparable performance compared to the conventional I-shape configuration.

References

- [1] Z. Q. Zhu, X. Chen, J. T. Chen, D. Howe and J. S. Dai, "Novel linear flux-switching permanent magnet machines," in Proc. Int. Conf. on Electrical Machines and Systems (ICEMS2011), pp. 2948-2953, 2011.
- [2] G. W. Mclean, "Review of recent progress in linear motors," in Proc. IEE- Electric Power Applications Conf., pp. 380-416, 1988.
- [3] M. Y. Wang, L. Y. Li, and D. H. Pan, "Analytical modelling and design optimization of linear synchronous motor with stair-step-shaped magnetic poles for electromagnetic launch applications," IEEE Trans. on Plasma Sci., vol. 40, no. 2, pp. 519-527, Feb. 2012.
- [4] S. M. Kazraji, and M. B. Sharifian, "Direct thrust force and flux control of a PM-linear synchronous motor using Fuzzy Sliding-Mode observer," Power Engineering and Electrical Engineering, vol. 13, no. 1, pp. 1-9, Mar., 2015.
- [5] D. Y. Chau, K.T. Cheng, Y. Fan, Y. Wang, Y. Hua, and Z. Wang, "Design and analysis of linear stator permanent magnet Vernier machines," IEEE Trans. on Magnetics, vol. 47, no. 10, pp. 4219-4222, 2011.
- [6] G. Stumberger, D. Zarko, M. T. Aydemir, and T. A. Lipo, "Design and comparison of linear synchronous motor and linear induction motor for electromagnetic aircraft launch system," in proc. International Electric Machines and Drives Conference, pp. 494-500, 2003.
- [7] W. Min, J. T. Chen, Z. Q. Zhu, Y. Zhu, M. Zhang and G. H. Duan, "Optimization and comparison of novel E-core and C-core linear switched flux PM machines," IEEE Trans. on Magnetic, vol. 47, no. 8, pp. 2134-2141, August, 2011.
- [8] E. Carraro, N. Bianchi, S. Zhang, M. Koch, "Permanent magnet volume minimization of spoke type fractional slot synchronous motor," IEEE Energy Conversion Congress and Exposition (ECCE), pp. 4180-4187, 2014.
- [9] C. Bianchini, F. Immovilli, E. Lorenzani, A. Bellini, and M. Davoli, "Review of design solutions for internal permanent-magnet machines cogging torque reduction," IEEE Trans. on Magnetics, vol. 48, no. 10, pp. 2685-2693, 2012.
- [10] Z. S. Du and T. A. Lipo, "Permanent magnet material and pulsating torque minimization in spoke type interior PM machines," IEEE Energy Conversion Congress and Exposition (ECCE), 2016.
- [11] C. F. Wang, J. X. Shen, Y. Wang, L. L. Wang and M. J. Jin, "A new method for reduction of detent force in permanent magnet flux-switching linear motors," IEEE Trans. on Magnetic, vol. 45, no. 6, pp.2843-2846, June, 2009.